Landsc Ecol (2024) 39:203
https://doi.org/10.1007/s10980-024-02005-9

RESEARCH ARTICLE

Using land surface phenology and information theory to assess and map complex landscape dynamics

Lars Y. Pomara · Danny C. Lee · Bjorn-Gustaf Brooks · William W. Hargrove

Received: 26 April 2024 / Accepted: 5 November 2024 / Published online: 19 November 2024

Abstract

Context Characterizing landscape ecological complexity and change requires integrated description of spatial and temporal landscape organization and dynamics, as suggested by the shifting mosaic concept. Remotely sensed land surface phenology allows the detection of even small differences among landscape patches and through time, allowing for the analysis of landscapes as shifting mosaics.

Objectives We sought to quantify aspects of the complex landscape behaviors that are implied by spatiotemporal variation in land surface phenology. We adapted an information-theoretic (IT) framework from ecosystem ecology to capture landscape-level spatiotemporal complexity and organization and map these properties across large areas.

Methods Phenology data were derived from remotely sensed, pixel-level time series of a vegetation greenness index, across a large portion of North America. We summarized multi-year, multi-pixel dynamics in transition matrices, calculated IT metrics from the matrices, and used matrix projection to quantify disequilibrium dynamics and long-term trajectories of the metrics.

Results Mapping the IT metrics and their disequilibria revealed gradients in the spatiotemporal complexity and organization of multi-year land surface phenology dynamics at continental to local scales. These gradients suggest influences of biophysical and biogeographic setting, ecological development and disturbances, land use, and other drivers of landscape ecological dynamics. The spatiotemporal IT metrics were influenced by both year-to-year dynamics and spatial landscape heterogeneity, but correlations with spatial and temporal complexity measures varied among the IT metrics. Landscapes showing the strongest disequilibrium dynamics were mostly in the western part of the continent and appeared to be associated with large-scale disturbances including severe fire, forest pathogens, climate variability, and land use change—important subjects for further study.

Conclusions This approach reveals novel features of the shifting landscape mosaic, with implications for understanding landscape resilience and sustainability. Resulting spatial data products describing long-term landscape dynamics have potential applications in broad-scale ecological modeling, monitoring, assessment, and prediction.

Supplementary Information The online version contains supplementary material available at https://doi.org/10.1007/s10980-024-02005-9.

L. Y. Pomara (✉) · D. C. Lee · W. W. Hargrove
Southern Research Station, USDA Forest Service, 200 WT Weaver Blvd, Asheville, NC 28804, USA
e-mail: lazarus.y.pomara@usda.gov

B.-G. Brooks
Carbon Solutions, LLC, 1041 Grand Ave #142, St. Paul, MN 55105-3002, USA

Keywords Information theory · Land surface phenology · Landscape dynamics · MODIS · Resilience · Shifting mosaic

Introduction

A landscape can be seen as a complex entity composed of smaller functional components, whose characteristics and organization change over time at multiple spatial and temporal scales. This 'shifting mosaic' view of internally complex, dynamic landscapes has long been a core concept for understanding landscape ecological processes, with broad implications for conservation and sustainability problems (Mayer et al. 2016; Spies and Turner 1999; Wu 2013; Wu and Loucks 1995). The shifting mosaic concept highlights the importance of studying spatial and temporal landscape structure and dynamics in a unified way, and it also implies an approach to monitoring spatiotemporal landscape dynamics quantitatively. For example, monitoring state transitions of individual pixels in a multi-pixel landscape over time, then compiling a matrix of transition probabilities, is a way to quantify a shifting landscape mosaic (Riitters et al. 2020, 2009). This relies on a classification system for pixel states (e.g., land cover/use types), with pixels assigned to a class in each time step so that transitions (e.g., from forest to urban cover/use) accumulate over time.

Remote sensing provides a primary basis for long-term and large-scale landscape monitoring. But to provide information about nuanced landscape ecological variability—for example, processes that occur within land use or ecosystem types—change detection needs to occur at an accordingly nuanced level (Kennedy et al. 2014; Pettorelli et al. 2014a, 2014b). An increasingly important approach for achieving this is the study of vegetation phenology—the timing of vegetation changes, often seasonal or cyclical—generalized in a remote-sensing context as Land Surface Phenology (LSP; Caparros-Santiago et al. 2021; Dronova and Taddeo 2022; Henebry and de Beurs 2013; Morisette et al. 2009). Gross changes in vegetation are tracked through many time steps within the annual cycle to characterize within-year phenology profiles, usually measured by a greenness index such as the Normalized Difference Vegetation Index (NDVI) or the Enhanced Vegetation Index (EVI), which are strongly correlated with gross primary productivity and biomass (Kerr and Ostrovsky 2003; Pettorelli et al. 2011, 2005). Multiple descriptive metrics can be derived from LSP profiles, including the degree of seasonality, seasonal timing benchmarks such as the beginning of the growing season, and productivity indicators such as mean or cumulative growing season greenness (Brooks et al. 2020; Cleland et al. 2007; Reed et al. 1994; Zhang et al. 2003). Such metrics are informative with respect to a wide variety of ecosystem and landscape properties and functions, and mapping them as spatial variables has advanced the study of landscape, ecosystem, ecoregion, and even biome diversity and distributions (Bolton et al. 2020; Buitenwerf and Higgins 2016; Polgar and Primack 2011; Radeloff et al. 2019; Silveira et al. 2022). The annual LSP profiles of pixels (or landscape patches) are influenced by biophysical context (e.g., climate and soils), vegetation composition, disturbances of various kinds (e.g., fire and forest insect and disease outbreaks), land use, and other dynamic factors (Brooks et al. 2020; Cleland et al. 2007; Frantz et al. 2022; Liang et al. 2021; Norman et al. 2017).

The capacity of remotely sensed LSP data to indicate ecologically nuanced year-to-year pixel dynamics makes it an ideal candidate for observing landscapes as shifting mosaics over longer time periods, but we are aware of no published examples of this. Choices about how multi-year, multi-pixel LSP dynamics might be quantified depend on broader objectives to inform sustainability and conservation problems, ecosystem management, or other targeted purposes. This study demonstrates an approach using information theory (IT) to quantify landscape-level LSP dynamics. To provide context for this approach in terms of broader objectives, a discussion of landscape resilience follows. Landscape resilience is a central concept linking landscape change to sustainability and conservation problems. Resilience has resisted simplistic definitions, and due to its contextual, contingent, and multivariate nature it may not be captured by any single quantitative measure (Angeler and Allen 2016; Folke 2006; Mayer 2008; McWethy et al. 2019; Quinlan et al. 2016). Nonetheless, informed judgements about resilience depend on repeatable measurements of landscape behavioral and organizational characteristics. We sought to develop such measurements as tools for studying landscape

resilience, geared to the systems-ecology approaches that are needed in this context.

Landscape resilience describes how the aggregate behavior of diverse landscape components and processes, experiencing varying kinds and degrees of change, influence sustainability outcomes such as the continued flow of ecosystem services or the maintenance of biodiversity (McWethy et al. 2019; Quinlan et al. 2016; Seidl et al. 2016; Wu 2013). Landscape sustainability can be thought of for these purposes as "the capacity of a landscape to consistently provide long-term, landscape-specific ecosystem services essential for maintaining and improving human well-being in a regional context and despite environmental and sociocultural changes" (Wu 2013). While resilience can be considered as a value-free characterization of system behavior, its association with sustainability usually also entails identifying particular system properties whose sustainability is considered desirable (Carpenter et al. 2001; Mayer 2008). Resilience emphasizes how thresholds, nonlinearities, disequilibria, and novelty in complex system dynamics may structure capacities for both sustainability and adaptation (Folke 2006; Scheffer et al. 2001; Wu 2013). Ecosystem growth, development, disturbance, and recovery play crucial roles—the complexity and organization of these processes are linked to a system's capacity to support sustainability goals (Levin and Lubchenco 2008). As the disturbance history of individual system components plays out through time, aggregate system behavior may be near a stable equilibrium, or it may drive shifts towards new states and novel dynamics. Such fundamental shifts may be inconsistent with some sustainability goals, but they may also be associated with adaptability (Elmqvist et al. 2003; McWethy et al. 2019; Seidl et al. 2016; Wu 2013).

Resilience theory has roots in ecosystem ecology (Folke 2006; Gunderson 2000), wherein ecosystems are viewed as complex systems—networks of biotic and abiotic components and processes with quantifiable, aggregate system dynamic properties (Holling 1973; Li 2000; McNaughton 1977). Ulanowicz (1986, 1997) followed others in adapting measures of system entropy from IT to quantify the complexity of energy flows and food web dynamics among organisms within an ecosystem (MacArthur 1955; Rutledge et al. 1976). Various IT measures have since been adapted to characterize landscape complexity, usually in relation to spatial composition and configuration (Nowosad and Stepinski 2019; Riitters et al. 2023), but sometimes for spatiotemporal analysis (Parrott 2010; Zaccarelli et al. 2013). Ulanowicz's (1986) framework is useful because it partitions the complexity of system dynamics into organized (predictable) and disorganized (unpredictable) components—the Mutual Information and Conditional Entropy, respectively. It also scales these to system productivity, resulting in metrics termed Ascendency and Overhead. While Ulanowicz' approach has not been widely used in landscape ecology, it is broadly applicable to a wide variety of systems (Ulanowicz 1997, 2003). It holds special appeal for interpreting system complexity in terms related to resilience, because the metrics help characterize a system's history of development and disturbance, and its capacity for change and adaptation (Costanza and Mageau 1999; Ulanowicz et al. 2009).

Our goal was to adapt IT metrics from ecosystem ecology to quantify landscape-level LSP composition and change, characterizing the observed spatiotemporal dynamics as aggregate, system-level properties. We compiled LSP year-to-year dynamics within multi-pixel landscapes, then mapped the resulting IT metric values for most of temperate North America. We expected to find coherent geographic variation in the complexity and organization of LSP dynamics, at continental to local (tens of kilometers) scales. More generally, we expected that the IT approach can reveal novel features of the shifting landscape mosaic, with potential to support assessments of landscape resilience.

Although not analyzed in this study, we also expected variation in the IT metrics to be relatable to a variety of environmental drivers, as well as outcomes such as the provisioning of ecosystem services. This is because the IT metrics, and the trajectories of landscape change they suggest, are ultimately determined by multiple drivers of the annual LSP states and state changes we studied. We did not analyze variation in the metrics relative to specific drivers, instead emphasizing the implications of the metrics as integrative measures of overall landscape behavior, particularly in resilience and sustainability contexts (Costanza and Mageau 1999; McWethy et al. 2019; Quinlan et al. 2016; Wu 2013). However, to better illustrate how the metrics can aid the study of specific drivers that may impact landscape resilience,

we also discuss some clear relationships to climate and land use/cover, and we provide two cases involving large-scale forest disturbances.

Methods

Our analysis began with a continental-scale dataset of pixel-level NDVI time series derived from the Moderate Resolution Imaging Spectroradiometer (MODIS) satellite system, resolved into annual LSP states (Brooks et al. 2020). We compiled transition matrices for multi-pixel landscapes from nearly two decades of annual transitions among the pixel-level LSP states, then calculated the IT metrics from the transition matrices. The metrics take on fixed values quantifying dynamics that have been summarized across the entire time period. But the observed transitions also suggest either stable (i.e., at dynamic equilibrium) or unstable complexity and organization. To examine this, we used matrix projections to compare the observed dynamics with projected equilibrium dynamics. This produced estimates of long-term trajectories of change—or disequilibria—in the IT metrics, given the observed dynamics. The following sections detail each of these steps in our analysis.

Annual phenological classification

Our approach to classify annual phenological states (Fig. 1) is reported in Brooks et al. (2020). While it was not part of the present analysis, generating phenological classes ('phenoclasses') was a basis for quantifying landscape LSP composition and change, so a review of these methods provides context for the present study. Briefly, it began with a 2000–2018 time series of NDVI values for MODIS pixels, each nominally 250 m^2, in North America between 20° and 50° latitude (Spruce et al. 2016). Daily to twice-daily data from the Aqua and Terra satellites were previously processed to produce a smoothed and gap-filled, max-composite time series reported at 8-day intervals, or 46 periods per year. This processed NDVI dataset has few missing values, minimizes cloud interference, and has been used extensively in LSP applications and research (Konduri et al. 2020; Norman et al. 2013; Spruce et al. 2019, 2011).

Each pixel's time series was plotted in polar space and segmented into phenological years that begin and end at the date of the mean antivector of the values, independent of calendar year (Brooks et al. 2017). Then eleven circular metrics were calculated by pheno-year, quantifying various aspects of the annual phenological cycle (Table 1; Fig. 1d). To enhance interpretability and reduce data volume, these annual metrics were subjected to a factor analysis resulting in four factors that explained 95% of the variance in the full dataset, and which described the three fundamental aspects of LSP: productivity, seasonality, and timing. One factor was associated with productivity, having high loadings for variables that quantify the magnitude of NDVI during the growing season. Another factor was associated with seasonality, having high loadings for the length of the growing season and the standard deviation of NDVI. Timing required two factors to fully describe, due to the circular nature of the annual cycle and the polar coordinate approach used to uniquely identify points along the cycle. These two factors had high loadings for variables expressing those timing points, including the beginning, middle, and end of the growing season relative to the Julian calendar.

Finally, a nonhierarchical k-means cluster analysis partitioned the four-dimensional factor space into 500 clusters (Brooks et al. (2020) discuss the motivation for this choice of the number of clusters to represent the range of LSP variability in the data). These clusters constitute a quantitative typology of LSP annual states that we refer to as phenoclasses (Fig. 1). This results in a phenoclass assignment for each pixel in each pheno-year, reducing the dynamics of each pixel to a series of annual state transitions from one phenoclass to another. A year-to-year phenoclass change indicates that the gross vegetation phenology, as defined by the four factors, has changed enough to suggest meaningful change in the vegetation (i.e., usually induced by disturbance, growth, or response to conditions such as drought stress (Brooks et al. 2020).

These states and transitions were the starting point for the present analysis. The transition from any given phenoclass to another represents a unique and defined change in some combination of productivity, seasonality, and timing. However, the present analysis does not track the specific character of every possible transition type—instead, it uses this diversity of transition types to quantify the degree, complexity, and

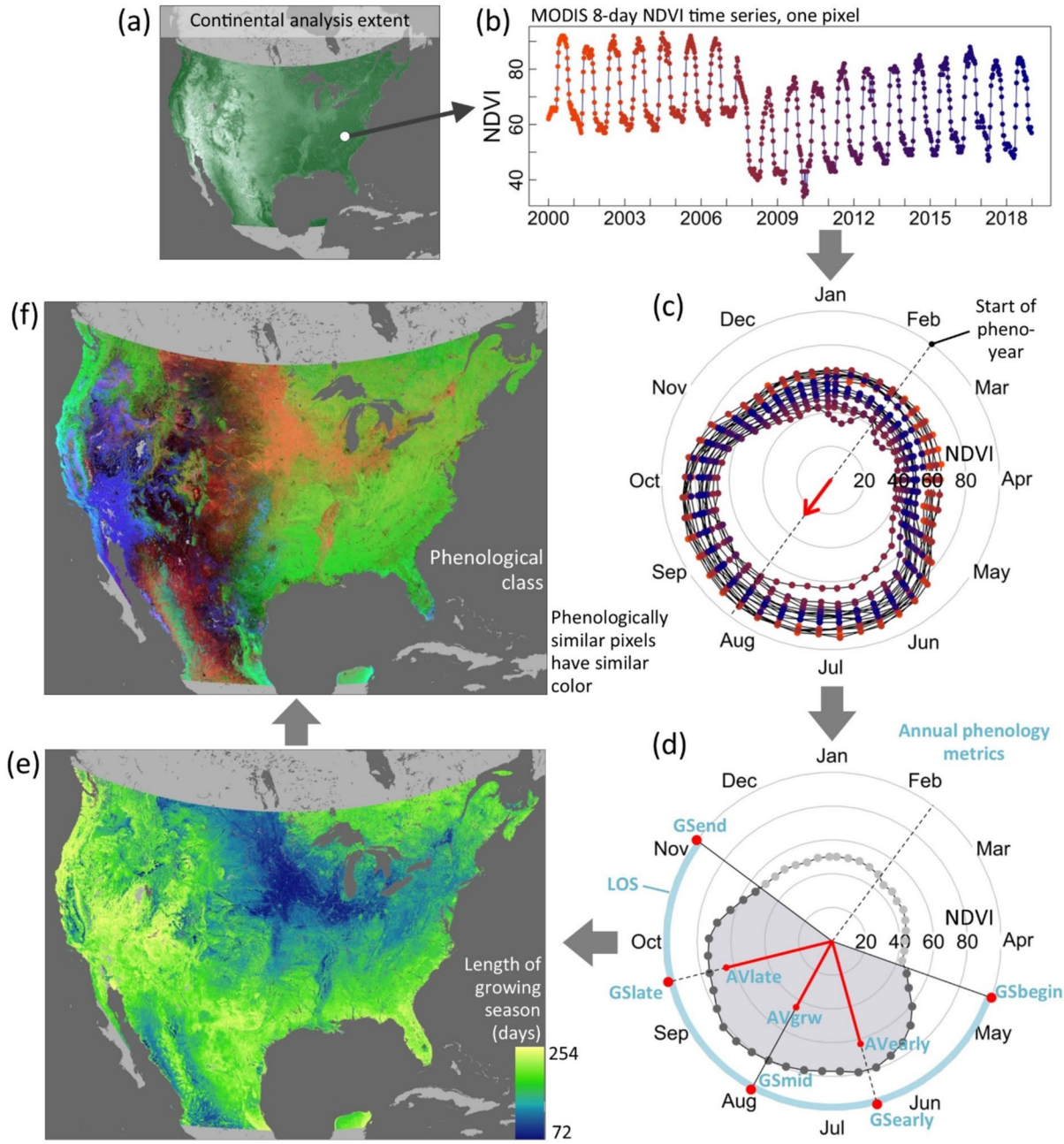

Fig. 1 Overview of land surface phenological classification based on annual phenology metrics, reported by Brooks et al. (2020). **a**, **b** Normalized Difference Vegetation Index (NDVI) time series with an 8-day sampling interval were developed for each MODIS pixel (~250×250 m2) across most of North America. Seasonality, disturbance, and recovery are evident in the example pixel. **c** The polar-plotted time series were segmented into phenological years based on their seasonality timing, with the start of the phenological year defined by the antivector of the data. **d** Polar metrics describing the annual phenology were calculated for each pixel in each year. Abbreviated metric names are linked to descriptions in Table 1 (mean and standard deviation of growing season NDVI are not shown here; they were calculated from the NDVI values between GSbegin and GSend). **e** The length of the growing season (LOS) is one metric, shown for illustration. Factor analysis reduced these metrics to four fundamental dimensions: seasonality, productivity, and two timing dimensions. **f** Phenological classes (phenoclasses) were created from the factors through cluster analysis. Phenoclasses are shown as an RGB color composite of the cluster centroid values for the three most important phenological factors. The phenoclass membership of a pixel may change from year to year

Table 1 Eleven LSP variables used to describe annual phenology based on pixel-level NDVI time series

Short name	Name	Units	Description
GSbegin	Beginning of growing season	Day	15% of cumulative annual NDVI
GSearly	Middle of early growing season	Day	32.5% of cumulative annual NDVI
GSmid	Middle of growing season	Day	50% of cumulative annual NDVI
GSlate	Middle of late growing season	Day	65% of cumulative annual NDVI
GSend	End of growing season	Day	80% of cumulative annual NDVI
LOS	Length of growing season	Days	Number of days between GSbegin and GSend
meanNDVIgrw	Average growing season NDVI	NDVI	Average NDVI during the growing season
stdNDVIgrw	Growing season NDVI variability	NDVI	Standard deviation of NDVI in the growing season
AVearly	Early growing season seasonality	NDVI	Length of the average vector for the early growing season
AVgrw	Growing season seasonality	NDVI	Length of the average vector for the growing season
AVlate	Late growing season seasonality	NDVI	Length of the average vector for the late growing season

Refer to Fig. 1 for an illustration of how each was calculated using a polar coordinate transformation approach

Day = Julian calendar day corresponding to the radial angle at which a given threshold occurs

Adapted from Brooks et al (2020)

organization of the overall LSP dynamics occurring within multi-pixel landscapes.

Spatial and temporal scale

We defined a landscape as a square group of adjacent MODIS pixels observed over a continuous multi-annual period, allowing for the analysis of spatiotemporal heterogeneity at the landscape level. We analyzed landscapes composed of 25 MODIS pixels in a 5 × 5 grid, 134 ha in total area. This landscape extent was essentially arbitrary—methods are the same for other extents—but we chose to illustrate metric calculations at a small landscape size to emphasize the resulting spatial gradients among landscapes at management-relevant scales and to minimize processing times. We used a sliding window approach with a window centered on every pixel, so that each pixel was assigned results for the surrounding 25-pixel landscape. We present results for North America based on 18 consecutive pheno-years beginning in calendar year 2000 (Brooks et al. 2020). The number of possible transitions (n_{st}) observed in a landscape was therefore $n_s(n_t - 1) = 425$, where n_s is the number of pixels or the spatial sample, and n_t is the number of pheno-years or the temporal sample.

Information-theoretic metrics

We built a transition matrix for each pixel based on its surrounding 25-pixel landscape, to quantify the observed phenoclass composition and year-to-year transitions. We did this by extracting the time series of phenoclass assignments for each included pixel and tabulating the frequencies of transitions from any phenoclass A to any phenoclass B (Fig. 2). Each cell in the matrix therefore identified a unique A-B transition type, and the matrix summarized the frequencies of phenoclasses and transition types in the landscape. This matrix was the basis for all subsequent calculations of IT metrics. All analyses were performed in R (R Core Team 2021).

Each pixel in a landscape could, in a given year, belong to any of the 500 possible phenoclasses, making the transition matrix potentially large. In practice the combination of phenoclasses found together in a given landscape and the observed transition types were far more constrained, because some phenoclasses only occur in certain regions, some transition sequences are highly improbable (e.g., a very low-NDVI to a very high-NDVI phenoclass from one year to the next), etc. Further, as described below, unobserved transition types had no influence on the IT metric calculations. Transition matrices were therefore constructed according to the phenoclasses actually observed in a given landscape.

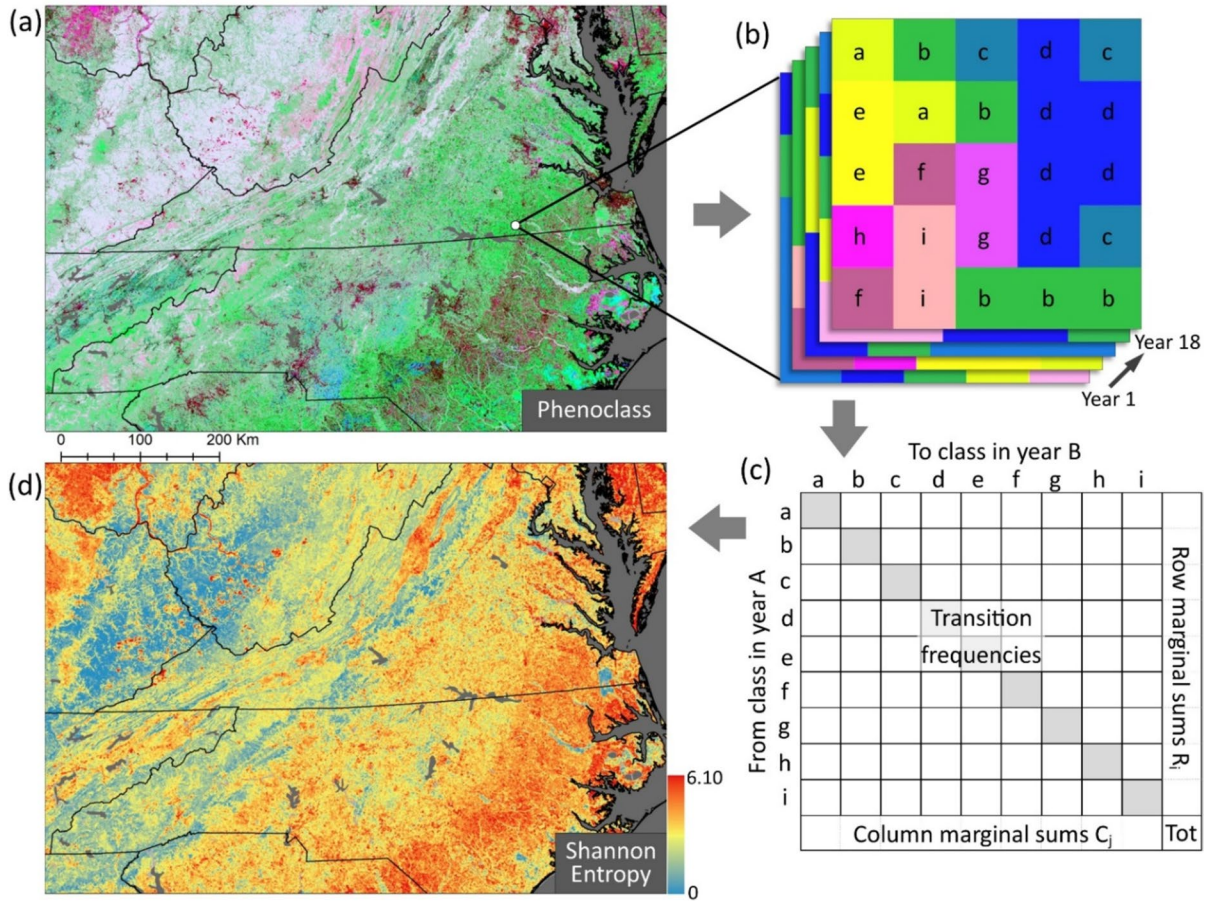

Fig. 2 Aspects of landscape spatiotemporal organization and behavior are quantified by calculating information-theoretic (IT) metrics from a transition matrix that summarizes inter-annual changes in land surface phenology. **a** Phenoclass membership data (Fig. 1f, shown here for the Mid-Atlantic region of the United States) are extracted for **b** a chosen landscape extent of contiguous MODIS pixels, for a continuous sequence of phenological years. In a 25-pixel, 18-year landscape there are 425 year-to-year transitions. **c** A transition matrix for each such landscape holds the frequencies of all inter-annual transitions from one phenoclass (rows; year A) to another (columns; year B) summarized for the multi-year period. Cells on the diagonal summarize transitions during which there was no phenoclass change between years. **d** Landscape IT metrics are calculated from the transition matrix, assigned to the center pixel, and mapped at MODIS spatial resolution. Each pixel contains information about the dynamics of the surrounding landscape

Our measure of overall landscape dynamic complexity was the Shannon Entropy index H, equivalent to system entropy, and widely used as a fundamental measure of complexity or diversity (Shannon 1948):

$$H(P) = -\sum_{i} \left(P_i \cdot \log_2 \left(P_i\right)\right) \quad (1)$$

where P are the probabilities associated with observed phenoclass transitions. Unobserved transition types ($P=0$) were entered in the sum as zeroes and did not influence the result. To calculate H for a given landscape, we summarized the data as follows. Let M be the transition matrix with elements $M_{i,j}$ recording the observed frequencies of transitions from phenoclass i in year t to phenoclass j in year $t+1$, across all observation years. Calculate the marginal (R=Row and C=Column) and total sums and probabilities:

$$R_i = \sum_j M_{i,j} \tag{2}$$

$$C_i = \sum_j M_{i,j} \tag{3}$$

$$total = \sum C \tag{4}$$

$$PA_i = \frac{R_i}{total} \tag{5}$$

$$PB_j = \frac{C_j}{total} \tag{6}$$

$$PAB_{i,j} = \frac{M_{i,j}}{total} \tag{7}$$

where A denotes the 'from' year t, and B denotes the 'to' year $t+1$. The Shannon Entropies of the 'from' and 'to' transition probabilities are then $HA = H(PA)$ and $HB = H(PB)$. We used their geometric mean:

$$meanH = \sqrt{(HA \cdot HB)} \tag{8}$$

The mean is useful because at the beginning of the full temporal sequence there is an initial 'from' year which is not a 'to' year, and likewise the final year is a 'to' but not a 'from'. Therefore, HA and HB typically have slightly different values, and meanH is informed by all years. Hereafter we refer to meanH simply as H.

Mutual information (MI) is a key measure of system organization and development, closely related to H (Rutledge et al. 1976; Steuer et al. 2002; Ulanowicz 1986). MI measures the degree to which knowledge about A influences the uncertainty in B (and vice versa). That is, MI estimates the predictability of the phenoclass distribution in a given year knowing the classifications of the same pixels in the previous (or subsequent) year. It is symmetrical with respect to A and B. The average MI for M across all years is:

$$MI = \sum_i \sum_j \left(PAB_{i,j} \cdot \log_2 \left(\frac{PAB_{i,j}}{PA_i \cdot PB_j} \right) \right) \tag{9}$$

Unobserved transition types were entered as zeroes and did not influence the result. The H and MI are both dimensionless informational quantities scaled in bits. The MI is always a fraction of H, quantifying the landscape dynamic complexity that is organized, i.e., LSP states are predictable given knowledge of prior states. The remaining fraction of H is the conditional entropy, $CE = H(B|A) = H - MI$, indicating the portion of the landscape complexity that is disorganized or unpredictable (Rutledge et al. 1976; Steuer et al. 2002; Ulanowicz 1986). We also calculated the proportion of H accounted for by MI, to quantify the degree of organized complexity relative to the overall complexity. Ulanowicz (1986) referred to this as Development, calculated as MI / H.

Additional IT metrics were introduced by Ulanowicz (1986, 1997) as a means of scaling H, MI, and CE to overall ecosystem activity or productivity. He estimated a scaling factor from the transition matrix as the total ecosystem throughput, by summing the energy transfers (i.e., transitions) in the system. A similar measure of total landscape dynamic activity (DA) can be calculated as the proportion of off-diagonal transitions in $M_{i,j}$, since our on-diagonal transitions are actually non-transitioning or stable phenoclasses:

$$DA = \sum_j PAB_{i,j} - \sum_j diagPAB_{i,j} \tag{10}$$

But the phenoclass transitions were not equivalent to trophic energy transfers, instead representing LSP dynamics driven by gross vegetation changes. Therefore, to instead scale to gross primary productivity, we used NDVI (Pettorelli et al. 2005). To estimate an overall productivity scaling factor, we used the mean NDVI across all MODIS pixel-year combinations in the landscape (meanNDVI).

Ulanowicz termed the system organization (MI) scaled by productivity as $Ascendency = MI \bullet throughput$. Our Ascendency calculation was therefore $Ascendency = MI \bullet meanNDVI$. Scaling CE in the same way produces system Overhead, $Overhead = CE \bullet meanNDVI$, and summing Ascendency and Overhead produces a metric corresponding to H and scaled to productivity, the Capacity: $Capacity = Ascendency + Overhead = H \bullet meanNDVI$. Note that the proportion of Capacity accounted for by Ascendency, i.e., Ascendency/Capacity, is equivalent to Development (Ulanowicz 1986). Metrics analogous to Ascendency, Overhead, and Capacity

but scaled to landscape dynamics irrespective of productivity could be calculated by substituting DA for meanNDVI, but this is not pursued here.

Spatial and temporal contributions to landscape complexity

Characteristics of $M_{i,j}$ are driven by both spatial and temporal heterogeneity, and as a result, the IT metrics are spatiotemporal descriptors. The spatial and temporal contributions can only be approximately decomposed, but two metrics help to indicate these contributions. Our approach was to assess temporal complexity by looking across years within pixels, and likewise to assess spatial complexity by looking across pixels within years. Temporal heterogeneity arises from the phenoclass transitions of individual pixels that populate the transition matrix, and the entropy of these pixel-level changes can be estimated by H using only the off-diagonal marginal sums, i.e., including only the matrix cells that represent inter-annual change between different phenoclasses. To scale this value appropriately it is multiplied by the proportion of the transitions that are in fact off-diagonal, i.e., DA. We term this the Temporal H, calculated as $H_{offdiag} \cdot DA$. While it quantifies the complexity of the phenoclass changes through time, the basis for its calculation is different from H and it cannot be strictly considered a component of H. Spatial heterogeneity also contributes to overall entropy because within-year phenoclass differences among pixels contribute to the composition of a landscape. This can be estimated by calculating H for phenoclasses observed in a given year, then taking the geometric mean across all years, i.e., the mean annual H. We term this the Spatial H, and the same caveats apply to its relation to H. This Spatial H accounts for landscape LSP composition, not configuration, and it is not equivalent to entropy-based measures of the complexity of landscape configuration (Nowosad and Stepinski 2019; Wang and Zhao 2018). We used Spatial H and Temporal H only as an approximate means to compare the relative contributions of spatial and temporal complexity to the IT metrics of primary interest.

Projecting landscape dynamics

Using projection matrices (Caswell 2001; Vandermeer 1981), we calculated the trajectory of change over time in landscape composition—i.e., change in the frequency distribution of phenoclasses present in the landscape—as a function of the observed dynamics. The current multi-annual phenoclass frequency distribution is represented by the marginal distribution of phenoclasses, R_i, over the observed period. The projection matrix m has elements $m_{i,j}$ equal to the probabilities of B, conditional on A:

$$PB|A_{i,j} = \frac{PAB_{i,j}}{PA_i} \tag{11}$$

where unobserved A resulted in zero values for the conditional probabilities. We then estimated the expected distribution D at y years of change as

$$D = m^y \cdot R_i \tag{12}$$

If the projection is carried out long enough, the phenoclass distribution will stabilize at a dynamic equilibrium. It is dynamic in the sense that inter-annual phenoclass transitions still occur, but at equilibrium they no longer alter the multi-annual phenoclass composition of the landscape. We obtained the equilibrium vector (EV) quantifying the equilibrium phenoclass distribution by calculating D for an arbitrarily large number of years, e.g., $y = 1000$ (or equivalently by examining the eigenvector of the projection matrix for the dominant eigenvalue). The goal was not to predict future conditions, but to assess the trajectory of the non-equilibrium landscape implied by the observed dynamics. Given that a landscape was not at equilibrium over the years observed, EV estimated the conditions it trended towards.

Observed landscapes may be close to dynamic equilibrium, or far from it. This can be measured by contrasting EV with the current phenoclass distribution R_i. To quantify this, we used the Kullback–Leibler (KL) divergence, an established IT measure of divergence between two probability distributions (Kullback 1997):

$$KL(EV, PA_i) = \sum_i \left(EV_i \cdot \log_2 \left(\frac{EV_i}{PA_i} \right) \right) \tag{13}$$

The Shannon entropy and mutual information at equilibrium can be calculated by combining EV with Eqs. 1 and 9:

$$H(EV) = -\sum_i \left(EV_i \cdot \log_2 \left(EV_i \right) \right) \tag{14}$$

$$MI(EV) = \sum_i \sum_j \left(\left(PB|A_{i,j} \cdot EV_j \right) \cdot \log_2 \left(\frac{PB|A_{i,j}}{EV_j} \right) \right) \quad (15)$$

Under equilibrium conditions, the Row and Column marginal probabilities are equivalent, and equal to EV, so it is unnecessary to calculate meanH(EV). The remaining IT metrics at equilibrium conditions can be calculated from H(EV) and MI(EV). For the NDVI-scaled metrics, commensurate meanNDVI and meanNDVI(EV) values were calculated as the mean of NDVI values for the phenoclasses present, weighted by their frequencies. We then used the difference between IT metric values under current conditions and equilibrium conditions (e.g., H(EV) – H) to quantify the trajectory of long-term increase or decrease implied by the observed dynamics—i.e., disequilibrium—for each of the metrics.

Metric maps and summaries

Table 2 lists the landscape metrics produced by our analysis. We generated gridded output for each metric at MODIS (250 m^2) spatial resolution, using the Raster package in R (Hijmans 2022), then developed maps using ArcGIS software (ESRI 2019). We also produced graphical summaries to examine metric value distributions, and we used Pearson correlation and simple linear regression to compare variation in the IT metrics to meanNDVI, Spatial H, and Temporal H. We used a spatially balanced, random sample of 25,000 landscapes across the study area for the data plots, correlations, and regressions. We do not present significance tests because the large sample size virtually guaranteed significant results at normal alpha levels, even for marginal correlations. The sampling scheme, and all maps, used the US National Atlas Equal Area projected coordinate system.

Local illustrations of landscape dynamics with known drivers

Local cases of landscapes with well-documented disturbance histories can help to interpret some drivers of variation in the IT metrics. These examples also help to illustrate how the metrics capture complex underlying LSP dynamics, in extreme cases where large-scale disturbances and post-disturbance

Table 2 Information-theoretic metrics developed to quantify spatiotemporal complexity and organization of landscape dynamics

Metric	Abbr	Unit	Description
Shannon Entropy	H	Bits	The total complexity of spatiotemporal dynamics. Quantifies the variety of phenoclasses and phenoclass transition types
Mutual Information	MI	Bits	The organized and predictable component of H. Quantifies regular or structured dynamics: knowledge of prior states allows prediction of subsequent states
Conditional Entropy	CE	Bits	The disorganized and unpredictable component of H (H–MI). Quantifies chaotic dynamics: prior states do not provide information about subsequent states
Development	–	Proportion	MI standardized with respect to H (MI/H or Ascendency/Capacity). The degree of organization, given the amount of complexity present
Capacity	–	Bits*ndvi	H scaled to productivity (H*ndvi)
Ascendency	–	Bits*ndvi	MI scaled to productivity (MI*ndvi)
Overhead	–	Bits*ndvi	CE scaled to productivity (CE*ndvi)
Dynamic activity	DA	Proportion	Degree of inter-annual variability; indicates the prevalence of short-term dynamics
Temporal H	–	Bits	Complexity of landscape changes over time
Spatial H	–	Bits	Complexity of within-year landscape composition
Equilibrium distance	KL	Bits	Divergence of the observed dynamics from equilibrium dynamics; gross measure of disequilibrium, implying a long-term trajectory of change
Equilibrium distance[1]	–		Difference between the equilibrium and observed values of an IT metric; indicates the long-term trajectory of the metric implied by the dynamics

[1]Equilibrium distance was calculated for each of the primary IT metrics (the first seven metrics listed); units are the same as the respective metric

The metrics are calculated from series of transitions over time between annual land surface phenology states, in a shifting landscape mosaic composed of multiple pixels

dynamics dominate the long-term LSP dynamics. We used two such cases from the eastern and western United States to interpret pixel-level NDVI time series, annual phenoclass compositions, and selected IT metrics. These examples highlight the potential for monitoring long-term dynamics as a cumulative outcome of complex landscape histories. The eastern case examines slow but pervasive impact from an invasive forest insect pest, and the western case examines fast, severe disturbance and subsequent regrowth associated with wildfire.

Results

Continental-scale maps of the IT metrics are shown in Figs. 3–5; the full map collection including metrics not shown in Figs. 3–5 is in Online Resource 1. The seven principal metrics (Entropy, Mutual Information, Conditional Entropy, Capacity, Ascendency, Overhead, and Development) showed spatially coherent pattern at continental and regional scales (Figs. 3 and 2). Some patterns were clearly associated with familiar geographic and biophysical gradients including climate, topography, and land use/land cover—quantifying these associations is beyond the scope of the current study but will be the subject of future work. Other patterns were less familiar, particularly those indicating unexpected similarity in IT metric values between landscapes that differ strongly in terms of the ecosystems present and other biophysical context.

Shannon Entropy (H), our measure of overall complexity, correlated more strongly with the Temporal H index than the Spatial H index (Fig. 4), indicating that H did not result only from spatial phenoclass heterogeneity, but was largely determined by phenoclass changes through time. Shannon Entropy was highest for landscapes with near average values for meanNDVI (Fig. 4). Landscapes with high H and

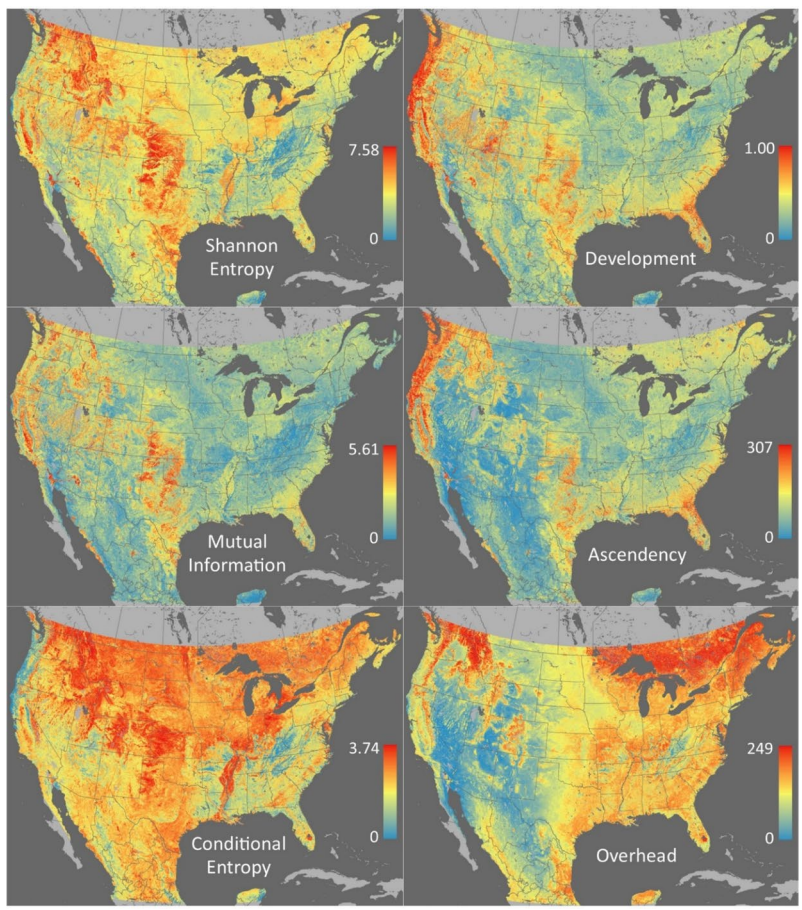

Fig. 3 Land surface phenology-based, information-theoretic metrics characterizing landscape dynamics and organization, estimated across 25-MODIS-pixel landscapes and over 18 phenological years corresponding approximately to 2000 – 2017. Color ramps are scaled to different ranges for the different metrics. Refer to Table 2 for metric descriptions

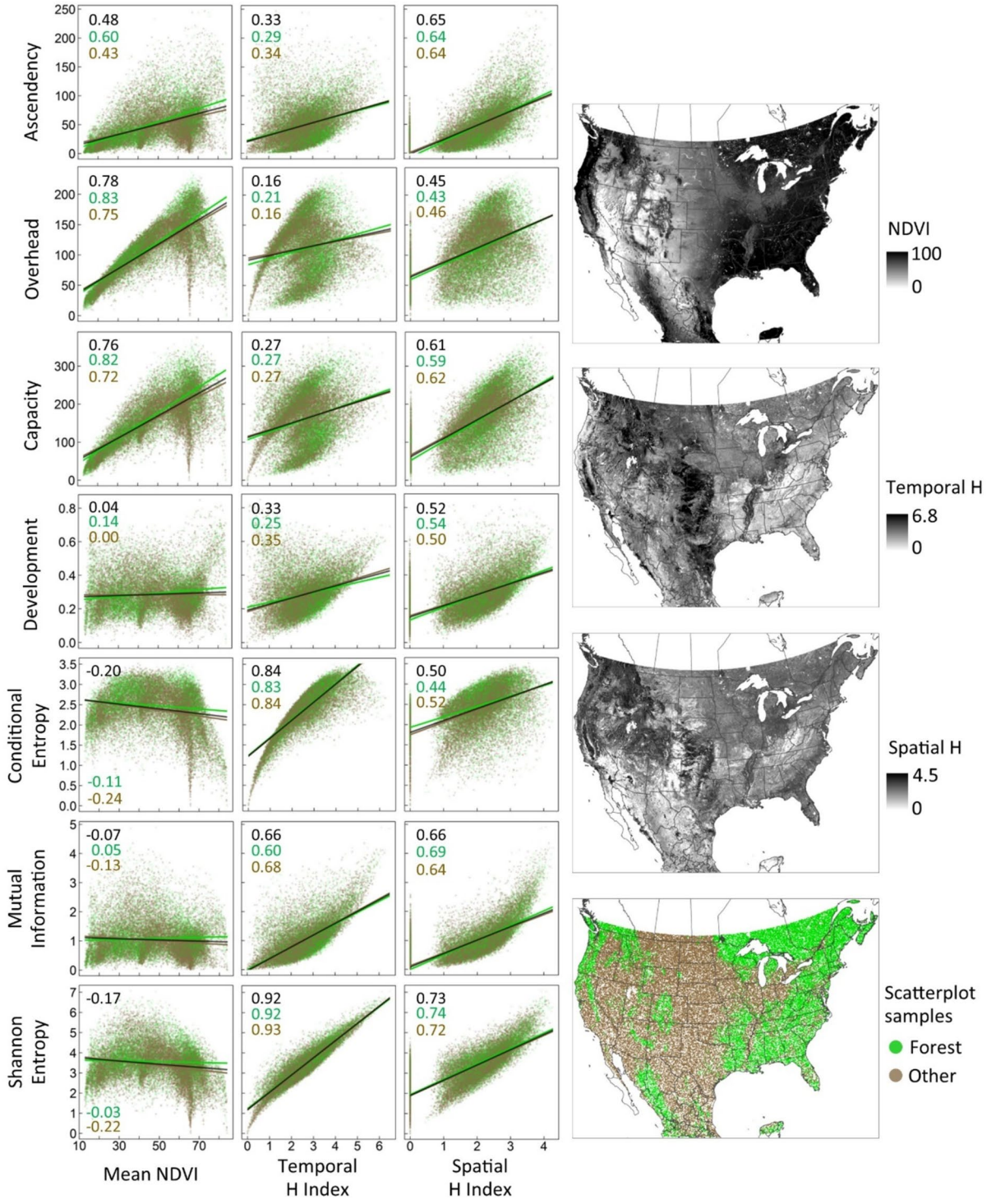

Fig. 4 Information-theoretic landscape metrics plotted in relation to the landscape mean NDVI, the complexity of changes through time as indicated by the Temporal H index, and spatial landscape complexity as indicated by the Spatial H index. Plots included a spatially balanced, random sample of 25,000 landscapes from across the study area. Point color distinguishes majority forest from majority non-forest landscapes. The Pearson correlation coefficients at the upper left of each plot and the linear regression slopes are color-coded for all points (black), forest, and non-forest

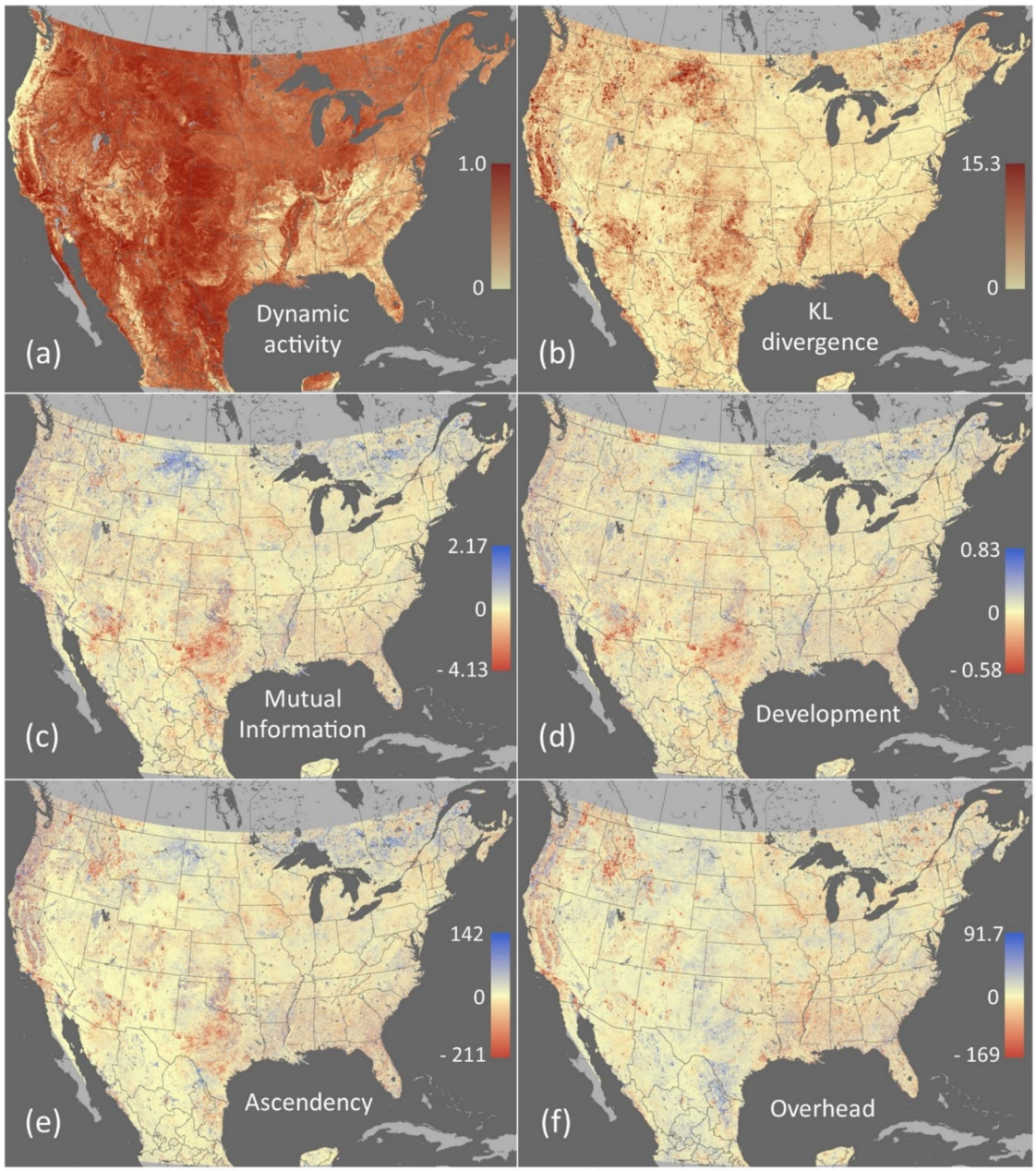

Fig. 5 Land surface phenology-based measures of the magnitude and direction of landscape dynamics, estimated across 25-MODIS-pixel landscapes and over 18 phenological years corresponding approximately to 2000 – 2017. **a** Dynamic Activity (DA) measures the proportion of annual phenoclass transitions that comprise a change in phenoclass rather than stasis; it is a measure of short-term, inter-annual dynamics. **b** The Kullback–Leibler (KL) Divergence estimates distance between the observed phenoclass composition (across the full time series) and the composition at dynamic equilibrium; it is a measure of the degree of long-term compositional change implied by the observed dynamics. While inter-annual phenoclass dynamics are common (**a**), only a fraction of high-DA landscapes are far from equilibrium (**b**). **c**–**f** Long-term trajectories in IT metrics implied by the disequilibrium dynamics expressed in (**b**). These trajectories indicate directional change in the complexity and organization of landscape dynamics

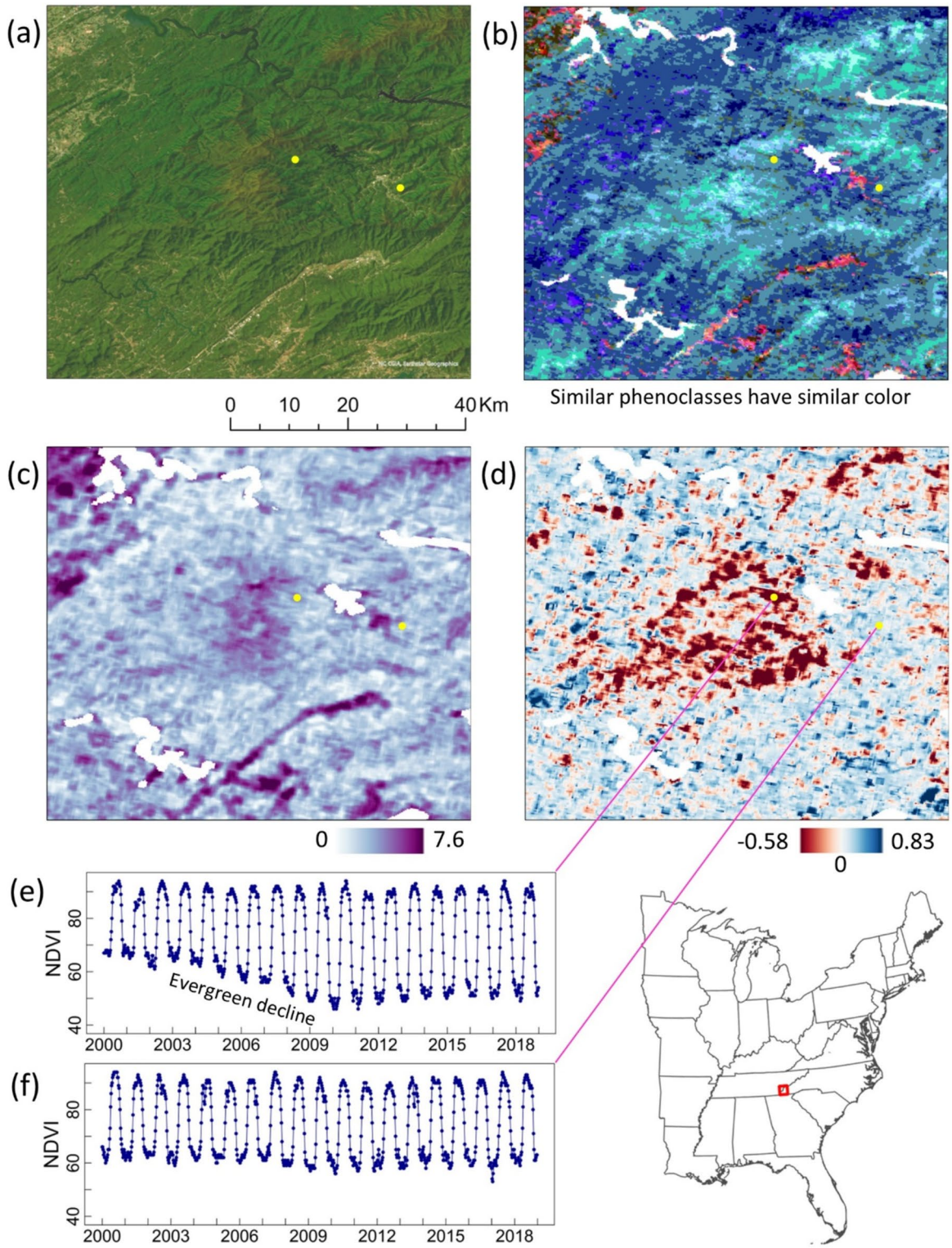
(a)
(b)
0 10 20 40Km
Similar phenoclasses have similar color
(c)
(d)
0 7.6
-0.58 0.83
0
(e)
NDVI
Evergreen decline
2000 2003 2006 2009 2012 2015 2018
(f)
NDVI
2000 2003 2006 2009 2012 2015 2018

◂**Fig. 6** Multi-year land surface phenology dynamics in mixed deciduous forest in the southern Appalachian Mountains affected by an invasive insect pathogen, the hemlock wooly adelgid. Widespread decline and mortality of two evergreen host tree species, eastern hemlock and Carolina hemlock, drove gradual winter NDVI decline during the first half of the study period. **a** True color air photo of an affected, mostly forested, subregion. The highest-elevation forests are in the center and northeastern parts of the image, and non-forest (developed and agricultural) areas are visible near the northwestern and southeastern corners. **b** Annual phenological classes during a single year, the pheno-year corresponding to 2017. **c** The Shannon Entropy (H) metric. The complexity of multi-pixel landscape dynamics across the full time series is higher in non-forest and in higher elevation forests. **d** Disequilibrium trajectory of the Development metric. The disequilibrium dynamics suggest local long-term decreases and increases in the metric. Landscapes with large reservoirs are removed (white). **e**, **f** Representative single-pixel NDVI time series showing (e) a pixel affected by hemlock decline and **f** an unaffected pixel. In this region, most landscapes showing a decreasing trajectory for Development typically contain many pixels similar to (**e**)

near average NDVI appeared to be common in agriculture- and rangeland-dominated regions, and at high elevations in montane regions such as the Rocky Mountains (Fig. 3). Shannon Entropy was low in both low-NDVI (e.g., Southwestern desert) and high-NDVI (e.g., forests in the Eastern US and Pacific Northwest) landscapes.

Conditional Entropy (CE), the unpredictable or chaotic component of H, correlated even more weakly than H with Spatial H, whereas MI, the predictable or organized component of H, correlated approximately equally with Spatial H and Temporal H (Fig. 4). This indicates that the disorganized, unpredictable component of landscape complexity was associated more strongly with temporal variability than with spatial heterogeneity. Shannon Entropy, MI, CE, and Development showed low Pearson correlation with meanNDVI. But as expected, the NDVI-scaled metrics Capacity, Ascendency, and Overhead were more strongly positively correlated with meanNDVI—and these correlations were stronger in forest than in non-forest landscapes (Fig. 4). All three of these productivity-scaled metrics were more strongly correlated with Spatial H than with Temporal H, in contrast to H, MI, and CE.

The dynamic activity (DA) index, the proportion of transitions that were off-diagonal, had its highest values in the Western and especially the Midwestern US. Its spatial pattern corresponded most closely to CE among the IT metrics (compare Fig. 5a to Fig. 3), further indicating the importance of inter-annual phenoclass variability as a driver of CE. However, DA did not correspond closely to KL divergence (Fig. 5). That is, strong inter-annual phenoclass variability did not necessarily imply, and in most landscapes did not result in, a pronounced trajectory of long-term phenoclass compositional change. In many high-DA landscapes in agricultural regions and rangelands, for example, pixels were likely to fluctuate among phenoclasses already present, rather than transition directionally toward locally novel states. These dynamic, but near-equilibrium (low-KL divergence) landscapes contrasted with high-KL divergence landscapes, which were concentrated in the western part of the continent and were more spatially isolated. This also had implications for the disequilibrium trajectories of the IT metrics as estimated through matrix projection (i.e., the difference between their observed and equilibrium values—Fig. 5c–f). Those trajectories showed spatially coherent pattern with many, spatially patchy, examples of both increase and decrease. At the continental scale, most landscapes showed values near zero, i.e., near dynamic equilibrium. While we do not present evidence beyond the spatial patterns visible in Fig. 5 and two illustrative local examples (Figs. 6 and 7), we suggest that many high-disequilibrium landscapes experienced large-scale disturbances during the study period or just prior to it, including impacts from severe wildland fire, forest pathogens, extended drought or other forms of increased climate variability (Brooks et al. 2020), and/or some forms of land use change.

Local illustrations of landscape dynamics with known drivers

Hemlock decline in Appalachian forests

Widespread decline and mortality of the evergreen conifer species eastern hemlock (*Tsuga canadensis*) and Carolina hemlock (*Tsuga caroliniana*) have been caused by hemlock wooly adelgid (*Adelges tsugae*), a non-native invasive insect pathogen in eastern North America (Ellison et al. 2018). In the southern Appalachian Mountains, the primary wave of hemlock decline occurred from approximately 2005 to 2010, having a more devastating impact than in most other affected regions (Ford et al. 2012; Krapfl et al. 2011; Vose et al. 2013). Hemlock is a widespread

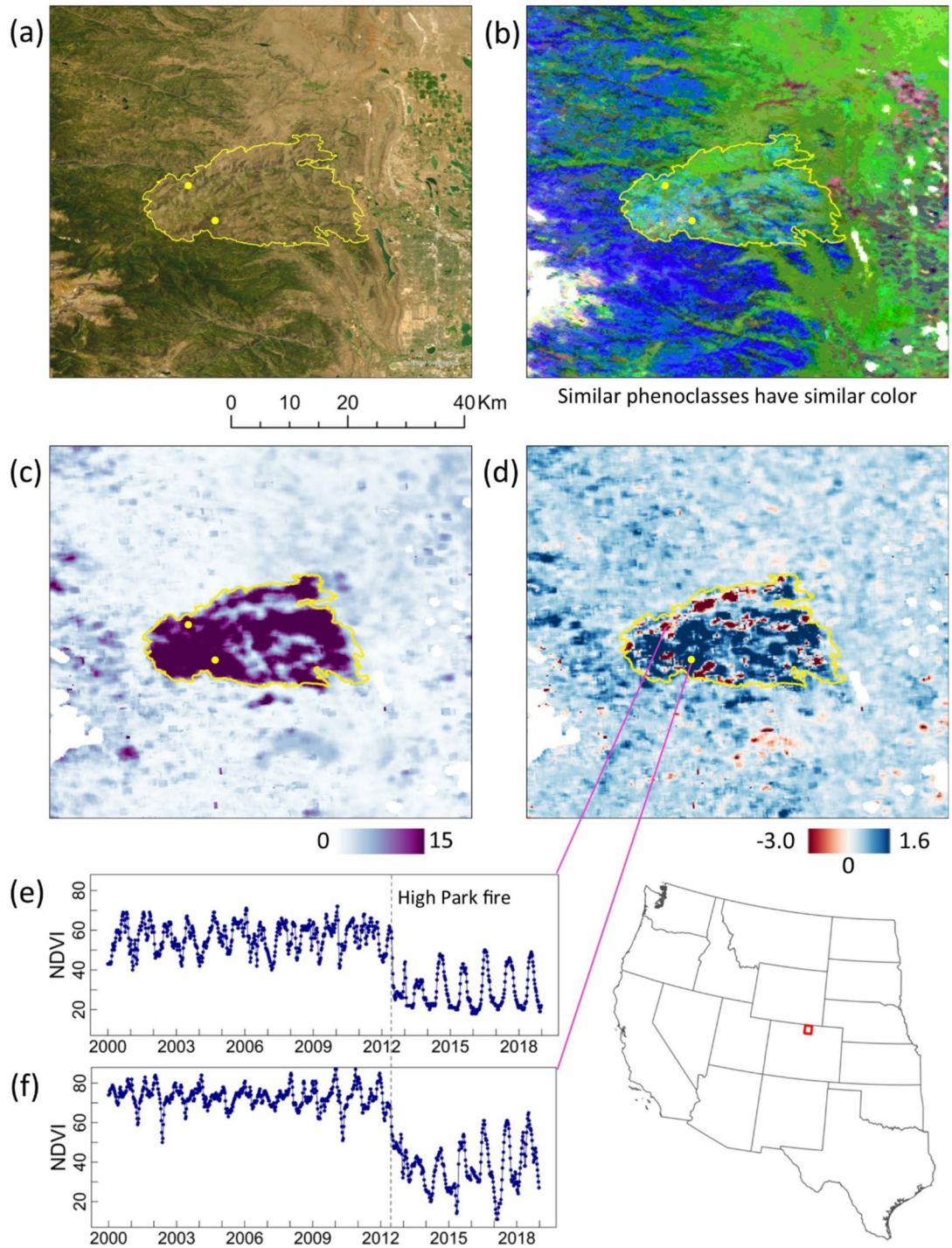

and common forest canopy tree in the region, and the gradual but pervasive disturbance associated with hemlock decline has contributed to the long-term complexity and organization of forest dynamics. In terms of pixel-level LSP, evergreen decline drove gradual reductions in winter NDVI in MODIS pixels where hemlock was a dominant component of mixed

◂**Fig. 7** Multi-year land surface phenology dynamics in a region impacted by high-intensity wildfire. **a** Post-fire true color air photo. The High Park fire occurred in summer 2012, west of Ft. Collins, Colorado. The city of Ft. Collins and nearby agricultural lands are in the eastern part of the image, with high-elevation conifer forest to the west. The fire perimeter is shown in yellow (Monitoring Trends in Burn Severity 2022). **b** Annual phenological classes during a single year, the pheno-year corresponding to 2017, with novel phenoclasses and local patchiness evident within the fire perimeter. **c** High values for Kullback–Leibler (KL) divergence suggest strong disequilibrium dynamics during the observation period, i.e., a trajectory towards novel conditions. **d** The disequilibrium trajectory of Conditional Entropy (CE) suggests local long-term decreases and increases in unpredictability within the fire perimeter. **e**, **f** Representative single-pixel NDVI time series. Many high burn severity areas showed evergreen forest-dominated phenology shifting to an herbaceous/shrub-dominated phenology with higher seasonality and lower productivity. Variation in the CE trajectory may be related to burn severity and recovery, and to differences in local pre-fire phenology. Landscapes with large reservoirs, and the highest elevation areas in the southwest corner, are removed (white)

deciduous forests, reducing mean productivity and increasing seasonality (Fig. 6e) (Norman et al. 2013).

Pixel-level phenoclasses in the region vary within forest, associated in part with elevation, while non-forest (mainly agricultural and urban) areas are more distinctive (Fig. 6a, b). At the landscape scale, the H metric (Fig. 6c) suggests that the complexity of landscape dynamics is greater in non-forest, and in high-elevation forests, but forests showing evergreen decline do not have obviously distinctive H values. However, the pixel-level dynamics associated with evergreen decline result in distinctive long-term disequilibrium dynamics at the landscape level (Fig. 6d). Strong within-forest pattern is evident in the disequilibrium trajectories—in particular, a decreasing trajectory in the Development metric in this region is primarily associated with evergreen decline. Most of the forest landscapes in Fig. 6d showing Development decrease contain many pixels with NDVI time series similar to that shown in Fig. 6e. This indicates long-term decline in the degree of organization and predictability associated with LSP dynamics in the affected forest landscapes.

Severe wildfire and post-fire dynamics

Wildland fire has complex impacts on LSP, causing shifts in annual timing, seasonality, and productivity that can depend on burn timing and severity, recovery history, and the type of vegetation affected (Wang and Zhang 2020). The potential for these shifts to influence the long-term complexity of landscape dynamics is suggested by widespread, disjunct patches of extreme values in KL divergence and disequilibria of the IT metrics in the western United States (Fig. 5b, e, f). The frequency, extent, and mean size of large wildfires in this region have all increased in recent decades (Costanza et al. 2023; Dennison et al. 2014; Weber and Yadav 2020). Based on clear spatial associations, we suggest that an important fraction of western landscapes showing extreme IT disequilibria experienced fire during or shortly before this study's observation period (Fig. 7).

The High Park fire burned approximately 350 km^2 during June of 2012 to the west of Ft. Collins, Colorado, along a gradient from conifer forest with varied tree species compositions at higher elevations to shrubland and rangeland at lower elevations (Coen and Schroeder 2015). Annual LSP across the region where the fire occurred is heterogenous, varying among and within forest, shrubland/grassland, agricultural, and urban areas (Fig. 7b). Within the fire perimeter, the phenoclasses present five years post-fire are distinctive from adjacent unburned forest, showing strong patchiness and locally novel phenoclasses. The KL metric further indicates strong disequilibrium of the observed LSP dynamics associated with the fire (Fig. 7c). The disequilibrium trajectory of CE highlights variation in the directionality of these dynamics (Fig. 7d), which we suggest is related to spatial variation in pre-fire vegetation type and phenology, burn severity, and post-fire phenology (Coen and Schroeder 2015). A strong proportion of landscapes within the burn perimeter showed evergreen forest-dominated LSP shifting to an herbaceous/shrub dominated LSP with lower productivity and greater seasonality (Fig. 7d, e). Among such wildfire landscapes, a trajectory of decreasing CE may be associated with irregular and less predictable pre-fire dynamics shifting to more regular and predictable post-fire dynamics (Fig. 7d), whereas the more widespread areas showing increasing CE may be associated with an opposing shift, i.e., regular-to-irregular recovery dynamics (Fig. 7e). These shifting dynamics suggest a reorganization of LSP spatiotemporal pattern that may develop further with vegetation recovery beyond the years included in our data.

Discussion

The IT metrics we generated show spatial patterns that are in many instances readily interpretable. Although not analyzed here, their associations with dominant climatic, topographic, vegetation type, and land use gradients are discernable at continental and more local scales. This is not surprising, since large-scale vegetation phenological characteristics frequently correspond with, and can be indicative of, those gradients (Bajocco et al. 2019; Bolton et al. 2020; Cleland et al. 2007; Silveira et al. 2022; Zhang et al. 2019). But these associations go beyond annual, pixel-level LSP profiles. The IT metrics reveal associated gradients in landscape-level LSP heterogeneity in both space and time. For example, forest landscapes in the southwestern United States show local spatial heterogeneity in phenoclasses, and the landscape composition of phenoclasses can be related to elevation, forest type composition, forest management, and wildlife habitat use (Hoagland et al. 2018). Agriculture provides another example—agricultural LSP differs from forest and rangelands, and pixel-level trends in annual seasonality, productivity, and timing can be driven by crop type changes (Konduri et al. 2020; Zhang et al. 2019). Beyond this, the IT metrics also suggest high complexity in agricultural landscapes relative to forest landscapes, at least at the scale of our analysis. Agricultural regions such as the Mississippi Alluvial Valley and California's Central Valley showed high H driven by both LSP spatial heterogeneity and temporal dynamics (Fig. 4). This is consistent with observations of high spatial and temporal landscape heterogeneity associated with diverse cropping systems, harvest schedules, agricultural parcel patterns, and land cover (Heintzman et al. 2024; Konduri et al. 2020).

There are other, less familiar large-scale patterns apparent in the IT metrics that are not readily relatable to obvious drivers, which we suggest probably derive from complex influences of multiple drivers on LSP dynamics over time. In these cases, multiple otherwise ecologically distinctive landscapes may be shown to have similar regimes of LSP dynamics (e.g., highly predictable or unpredictable dynamics), and conversely, multiple landscapes with similar annual LSP properties may behave quite differently over longer time periods. In such cases, the IT metrics may capture spatiotemporal landscape properties that are difficult to recover from combinations of more traditional spatial or Earth observation data such as land use/land cover, climate, and topographic data, or from change or trend analysis at the pixel level alone (Kennedy et al. 2014; Pfeifer et al. 2012). For this reason, we expect that there is novel information in the IT metrics which can be useful in a variety of applications wherein quantifying landscape dynamic regimes can complement other landscape data. These may include assessing ecosystem dynamics and resilience modeling (Chambers et al. 2019; Dronova and Taddeo 2022; Trumbore et al. 2015); assessing ecological impacts of climate change and various other kinds of ecological risk assessment (Mayer et al. 2016; Wang and Zhang 2020); ecosystem service modeling and assessment (Müller 2005; Pomara and Lee 2021; Rieb et al. 2017); and species and ecosystem distribution modeling and habitat suitability modeling (Franklin 2010; Hoagland et al. 2018; Ponti and Sannolo 2022).

In each of these areas LSP-based measures of landscape dynamics may improve modeling and prediction, by providing landscape ecological links between stressors such as climate change and the ecosystem services, biodiversity, and other values that they impact. These impacts can be direct, such as physiological stress on vegetation from chronic drought, but indirect impacts of climate change are also pervasive, involving more complex system pathways (Daniels et al. 2011; Weiskopf et al. 2020). It may not be practical to measure all components of such pathways, but more synoptic measures of landscape dynamic regimes and how these regimes change over time and space may 'stand in' by quantifying the most relevant system-level variability. For example, we suspect that climate variability represents one driver of variation in the IT metrics within ecosystem types such as forests. In turn, the metrics could prove to be useful predictors of variation in an ecosystem service such as clean water supply from forest watersheds, which is impacted by variable forest condition and cover (Caldwell et al. 2023; Smith et al. 2011). We expand on this in the following discussion of landscape resilience.

Landscape resilience

The potential of the IT metrics for studying landscape resilience follows several premises that link the metrics to key aspects of complex system behavior.

Landscapes, as complex ecological systems, can be expected to become more ascendent (sensu Ulanowicz 1986) in the absence of disturbance, filling in with vegetation to the extent possible given local constraints (climate, soils, land use, etc.) and becoming more predictable so long as they remain relatively undisturbed (Müller 2005). Ascendency implies growth, development, and organization—but high-ascendency, high-MI, predictable systems may also be brittle in the sense that they are not readily recoverable following major disturbance (Holling 1973).

System uncertainty, quantified by the CE and overhead metrics, is related to random perturbations and to system redundancies (transitions from two or more different states to the same subsequent state, and vice versa). Disturbances of various kinds work against growth and development, altering vegetation in typically more drastic and unpredictable ways, usually introducing increased uncertainty. In extreme cases unpredictable dynamics may be driven by frequent, compounding disturbances leading to system degradation. But redundancies can also provide flexibility and adaptability, allowing for continuity of system functions despite turnover in system states or components (Holling 1973; Ulanowicz et al. 2009).

In general, a mixture of uncertainty and ascendency is present in overall system complexity. One expects high uncertainty where disturbances and redundancies are prevalent, and high ascendency where growth and development dominate. It has been suggested that the presence of both of these tendencies together in ecological systems confers adaptive capacity and resilience up to some limit (Costanza and Mageau 1999; Parrott 2010; Ulanowicz 2009). But if these limits exist—for example, a threshold or rate at which increasing system uncertainty ceases to confer adaptive capacity and begins to confer degradation—they are unlikely to be known for most applied cases, and they may be highly context dependent and difficult to generalize (Johnstone et al. 2016; Ulanowicz et al. 2009).

For this reason, establishing relationships between IT metrics and landscape resilience is likely to depend on (1) additional knowledge of landscape setting and disturbance history, and (2) well-defined resilience targets such as the sustainability of system processes, ecosystem services, or biodiversity—i.e., resilience of what, to what (Carpenter et al. 2001). For example, a working hypothesis based on the theoretical expectations outlined above might suggest that the sustainability of ecosystem services under conditions of frequent disturbance corresponds with a predictable ratio of ascendency to overhead—at least within particular domains defined by biophysical setting, ecosystem type, or other criteria (Ulanowicz et al. 2009).

Testing this working hypothesis is a potential application of the IT metrics that could advance our understanding of dynamic landscapes and their implications for resilience. The formulation of the IT metrics as large-scale data products such as those we have presented allows their comparison with other data quantifying disturbances and ecosystem services, potentially establishing an operational role for LSP monitoring in resilience assessment. Using LSP to explore interactions among disturbance, recovery, uncertainty, ascendency, and other system behaviors may lead to repeatable measures for assessing landscape resilience, even given important context dependencies (Carpenter et al. 2001; Quinlan et al. 2016).

Further exploring shifting landscape mosaics

There are multiple ways in which the IT approach we present could be applied to spatiotemporal data to further characterize the complexity and organization of dynamics, and to examine potential sensitivities in the analytical approach. The metrics are likely to display scale dependencies, which can be explored by recalculating them at smaller and larger landscape extents (number of pixels), spatial grains (size of pixels), and across shorter and longer time periods. The degree of typological distinction chosen when generating phenoclasses—i.e., the total number of phenoclasses—can also influence the magnitude of observed dynamics, although our initial explorations (not reported here) suggest that relative differences among landscapes in IT metric values are robust across reasonable variation in the fineness or coarseness of phenoclasses, so long as their number is sufficiently large.

The landscapes for which the metrics are calculated could be delineated differently to address research goals defined around spatial units such as watersheds or forest management units. Pixels can also be aggregated into ‘landscapes’ by ecological similarity regardless of location, e.g., bottomland hardwood vs. upland pine forest pixels,

or even by phenological characteristics (Hargrove and Hoffman 2004). This would help characterize the landscape dynamic regimes of different system types and may provide insights into the drivers of their dynamics. The approach we describe can also be used with different data types, so long as the temporal sampling density is adequate to describe annual profiles. For example, weather data are typically available with dense (e.g., daily) sampling, from which annual descriptors such as temperature and precipitation seasonality are commonly calculated. Information-theoretic metrics derived from such data could help quantify the complexity and organization of interannual climate variability, as well as the stability of such dynamics over longer timeframes.

A limitation of our analysis is that it ignores the spatial configuration or arrangement of LSP classes within landscapes. Spatial composition and configuration each contribute to spatial complexity, and both are fundamental concerns in landscape ecology. Multiple recent studies have quantified landscape configurational entropy using different methods, some using Shannon entropy based in information theory (Nowosad and Stepinski 2019; Wang and Zhao 2018), and some using Boltzmann entropy based in thermodynamics (Cushman 2016, 2021; Gao and Li 2019). Developing approaches that integrate the composition and configuration of landscape components in both space and time is a rich frontier for understanding landscape complexity and organization (Parrott 2010).

More generally, observed LSP dynamics may be assessed at landscape scales using a wide variety of approaches. LSP defines pixel characteristics that fluctuate with changes in the amount, composition, condition, growth, disturbance, and recovery of vegetation. Because of these sensitivities, LSP is emerging as a primary approach for ecologically nuanced landscape characterization from remotely sensed data. Separately, a wide variety of metrics have been developed to describe aspects of landscape pattern and change over time in terms of patch dynamics, gradient analysis, and other approaches (Costanza et al. 2019; Gustafson 1998, 2019). As LSP data from various remote sensing platforms become more widely available, and as longer LSP time series accumulate, it will be useful to explore how various metrics beyond those we have examined may be adapted to LSP data to describe landscape ecological pattern and process.

Landscape dynamics assessment tool

The multi-annual IT metrics and their trajectories, as well as the annual LSP variables that underpin them (Brooks et al. 2020), constitute a large, interrelated set of LSP data products for monitoring and interpreting spatiotemporal landscape ecological pattern and change. They can potentially aid the investigation of properties such as landscape resilience that involve complex dynamics over time, and may have broad environmental science applications. But they are time consuming and resource demanding to calculate. This barrier is partly addressed by the Landscape Dynamics Assessment Tool (LanDAT; https://landat.org). LanDAT summarizes the data development process and allows users to view the full suite of data products and the associated pixel-level NDVI time series in an interactive map environment with other geographic information. The annual phenoclass data used as inputs in this study, and the IT metric results, are available via LanDAT for download in raster format (also see Data Availability statement).

Acknowledgements NASA and Oak Ridge National Laboratories provided smoothed and gap-filled MODIS NDVI time series data. The National Environmental Modeling and Analysis Center (NEMAC) at the University of North Carolina-Asheville maintains the LanDAT online tool. B.-G. Brooks held an appointment to the USDA Forest Service Research Participation Program administered by the Oak Ridge Institute for Science and Education (ORISE), through an interagency agreement between the U.S. Department of Energy and the USDA.

Author contributions All authors contributed to the study conception and design, initiated by D.C.L. Data processing and analysis were performed by L.Y.P. and B.-G.B. The first draft of the manuscript was written by L.Y.P., and all authors commented on previous versions of the manuscript. All authors read and approved the final manuscript.

Funding Funding provided by the Eastern Forest Environmental Threat Assessment Center, USDA Forest Service.

Data availability The datasets generated and used in this study, i.e., the annual phenoclass rasters for North America that were used to compile landscape LSP dynamics, are available at https://landat.org/maps. Most of the analysis results are also available in raster format at the same location.

Declarations

Competing interests The authors declare no competing interests.

References

Angeler DG, Allen CR (2016) Quantifying resilience. J Appl Ecol 53(3):617–624

Bajocco S, Ferrara C, Alivernini A, Bascietto M, Ricotta C (2019) Remotely-sensed phenology of Italian forests: going beyond the species. Int J Appl Earth Obs Geoinf 74:314–321

Bolton DK, Gray JM, Melaas EK, Moon M, Eklundh L, Friedl MA (2020) Continental-scale land surface phenology from harmonized Landsat 8 and Sentinel-2 imagery. Remote Sens Environ 240:111685

Brooks B-GJ, Lee DC, Pomara LY, Hargrove WW (2020) Monitoring broadscale vegetational diversity and change across North American landscapes using land surface phenology. Forests 11(6):606

Brooks BGJ, Lee DC, Pomara LY, Hargrove WW, Desai AR (2017) Quantifying seasonal patterns in disparate environmental variables using the PolarMetrics R package. 2017 IEEE international conference on data mining workshops (ICDMW):296–302

Buitenwerf R, Higgins SI (2016) Convergence among global biogeographical realms in the physiological niche of evergreen and deciduous vegetation. Global Ecol Biogeogr 25(6):704–715

Caldwell PV, Martin KL, Vose JM et al (2023) Forested watersheds provide the highest water quality among all land cover types, but the benefit of this ecosystem service depends on landscape context. Sci Total Environ 882:163550

Caparros-Santiago JA, Rodriguez-Galiano V, Dash J (2021) Land surface phenology as indicator of global terrestrial ecosystem dynamics: a systematic review. ISPRS J Photogramm Remote Sens 171:330–347

Carpenter S, Walker B, Anderies JM, Abel N (2001) From metaphor to measurement: resilience of what to what? Ecosystems 4(8):765–781

Caswell H (2001) Matrix population models. Sinauer Associates Inc, Sunderland

Chambers JC, Allen CR, Cushman SA (2019) Operationalizing ecological resilience concepts for managing species and ecosystems at risk. Front Ecol Evol. https://doi.org/10.3389/fevo.2019.00241

Cleland EE, Chuine I, Menzel A, Mooney HA, Schwartz MD (2007) Shifting plant phenology in response to global change. Trends Ecol Evol 22(7):357–365

Coen JL, Schroeder W (2015) The High Park fire: Coupled weather-wildland fire model simulation of a windstorm-driven wildfire in Colorado's Front Range. J Geophys Res Atmos 120(1):131–146

Costanza R, Mageau M (1999) What is a healthy ecosystem? Aquat Ecol 33(1):105–115

Costanza JK, Riitters K, Vogt P, Wickham J (2019) Describing and analyzing landscape patterns: where are we now, and where are we going? Landscape Ecol 34(9):2049–2055

Costanza JK, Koch FH, Reeves M et al (2023) Disturbances to forests and rangelands. In: US department of agriculture, forest service. 2023. Future of America's Forest and Rangelands: Forest Service 2020 Resources Planning Act Assessment., Gen. Tech. Rep. WO-102. U.S. Department of Agriculture, Forest Service, Washington

Cushman SA (2016) Calculating the configurational entropy of a landscape mosaic. Landsc Ecol 31(3):481–489

Cushman SA (2021) Generalizing Boltzmann configurational entropy to surfaces, point patterns and landscape mosaics. Entropy 23(12):1616

Daniels LD, Maertens TB, Stan AB, McCloskey SPJ, Cochrane JD, Gray RW (2011) Direct and indirect impacts of climate change on forests: three case studies from British Columbia. Can J Plant Path 33(2):108–116

Dennison PE, Brewer SC, Arnold JD, Moritz MA (2014) Large wildfire trends in the western United States, 1984–2011. Geophys Res Lett 41(8):2928–2933

Dronova I, Taddeo S (2022) Remote sensing of phenology: towards the comprehensive indicators of plant community dynamics from species to regional scales. J Ecol 110(7):1460–1484

Ellison AM, Orwig DA, Fitzpatrick MC, Preisser EL (2018) The past, present, and future of the hemlock woolly adelgid (*Adelges tsugae*) and its ecological interactions with eastern hemlock (*Tsuga canadensis*) forests. Insects 9(4):172

Elmqvist T, Folke C, Nyström M et al (2003) Response diversity, ecosystem change, and resilience. Front Ecol Environ 1(9):488–494

ESRI (2019) ArcGIS Release 10.7.1. Environmental Systems Research Institute, Redlands

Folke C (2006) Resilience: the emergence of a perspective for social–ecological systems analyses. Glob Environ Change 16(3):253–267

Ford CR, Elliott KJ, Clinton BD, Kloeppel BD, Vose JM (2012) Forest dynamics following eastern hemlock mortality in the southern Appalachians. Oikos 121(4):523–536

Franklin J (2010) Moving beyond static species distribution models in support of conservation biogeography. Divers Distrib 16(3):321–330

Frantz D, Hostert P, Rufin P, Ernst S, Röder A, van der Linden S (2022) Revisiting the past: replicability of a historic long-term vegetation dynamics assessment in the era of big data analytics. Remote Sens 14(3):597

Gao P, Li Z (2019) Computation of the Boltzmann entropy of a landscape: a review and a generalization. Landsc Ecol 34(9):2183–2196

Gunderson LH (2000) Ecological resilience–in theory and application. Annu Rev Ecol Syst 31:425–439

Gustafson EJ (1998) Quantifying landscape spatial pattern: what is the state of the art? Ecosystems 1(2):143–156

Gustafson EJ (2019) How has the state-of-the-art for quantification of landscape pattern advanced in the twenty-first century? Landsc Ecol 34(9):2065–2072

Hargrove WW, Hoffman FM (2004) Potential of multivariate quantitative methods for delineation and visualization of ecoregions. Environ Manage 34(1):S39–S60

Heintzman LJ, McIntyre NE, Langendoen EJ, Read QD (2024) Cultivation and dynamic cropping processes impart land-cover heterogeneity within agroecosystems: a metrics-based case study in the Yazoo-Mississippi Delta (USA). Landscape Ecol 39(2):29

Henebry GM, de Beurs KM (2013) Remote sensing of land surface phenology: a prospectus. In: Schwartz MD (ed) Phenology: an integrative environmental science. Springer, Dordrecht, pp 385–411

Hijmans RJ (2022) Raster: geographic data analysis and modeling. R package version 3.5–15. https://CRAN.R-project.org/package=raster.

Hoagland SJ, Beier P, Lee D (2018) Using MODIS NDVI phenoclasses and phenoclusters to characterize wildlife habitat: Mexican spotted owl as a case study. For Ecol Manage 412:80–93

Holling CS (1973) Resilience and stability of ecological systems. Annu Rev Ecol Syst 4:1–23

Johnstone JF, Allen CD, Franklin JF et al (2016) Changing disturbance regimes, ecological memory, and forest resilience. Front Ecol Environ 14(7):369–378

Kennedy RE, Andréfouët S, Cohen WB et al (2014) Bringing an ecological view of change to Landsat-based remote sensing. Front Ecol Environ 12(6):339–346

Kerr JT, Ostrovsky M (2003) From space to species: ecological applications for remote sensing. Trends Ecol Evol 18(6):299–305

Konduri VS, Kumar J, Hargrove WW, Hoffman FM, Ganguly AR (2020) Mapping crops within the growing season across the United States. Remote Sens Environ 251:112048

Krapfl KJ, Holzmueller EJ, Jenkins MA (2011) Early impacts of hemlock woolly adelgid in *Tsuga canadensis* forest communities of the southern Appalachian Mountains. J Torrey Bot Soc 138(1):93–106

Kullback S (1997) Information theory and statistics. Dover Publications, Mineola

Levin SA, Lubchenco J (2008) Resilience, robustness, and marine ecosystem-based management. Bioscience 58(1):27–32

Li B-L (2000) Why is the holistic approach becoming so important in landscape ecology? Landsc Urban Plann 50(1–3):27–41

Liang L, Henebry GM, Liu L, Zhang X, Hsu L-C (2021) Trends in land surface phenology across the conterminous United States (1982–2016) analyzed by NEON domains. Ecol Appl 31(5):e02323

MacArthur R (1955) Fluctuations of animal populations and a measure of community stability. Ecology 36(3):533–536

Mayer AL (2008) Strengths and weaknesses of common sustainability indices for multidimensional systems. Environ Int 34(2):277–291

Mayer AL, Buma B, Davis A et al (2016) How landscape ecology informs global land-change science and policy. Bioscience 66:458–469

McNaughton SJ (1977) Diversity and stability of ecological communities: a comment on the role of empiricism in ecology. Am Nat 111:515–525

McWethy DB, Schoennagel T, Higuera PE et al (2019) Rethinking resilience to wildfire. Nat Sustain 2:797–804

Monitoring Trends in Burn Severity (2022) Burned areas boundaries dataset. MTBS Project, USDA Forest Service/U.S. Geological Survey. https://www.mtbs.gov/index.php/direct-download

Morisette JT, Richardson AD, Knapp AK et al (2009) Tracking the rhythm of the seasons in the face of global change: phenological research in the 21st century. Front Ecol Environ 7(5):253–260

Müller F (2005) Indicating ecosystem and landscape organisation. Ecol Indic 5(4):280–294

Norman SP, Hargrove WW, Christie WM (2017) Spring and autumn phenological variability across environmental gradients of Great Smoky Mountains National Park, USA. Remote Sens 9(5):407

Norman SP, Hargrove WW, Spruce JP, Christie WM, Schroeder SW (2013) Highlights of satellite-based forest change recognition and tracking using the ForWarn System. Gen. Tech. Report SRS-180. U.S. Department of Agriculture, Forest Service, Southern Research Station, Asheville

Nowosad J, Stepinski TF (2019) Information theory as a consistent framework for quantification and classification of landscape patterns. Landsc Ecol 34(9):2091–2101

Parrott L (2010) Measuring Ecological Complexity. Ecol Indic 10(6):1069–1076

Pettorelli N, Vik JO, Mysterud A, Gaillard J-M, Tucker CJ, Stenseth NC (2005) Using the satellite-derived NDVI to assess ecological responses to environmental change. Trends Ecol Evol 20(9):503–510

Pettorelli N, Ryan S, Mueller T et al (2011) The normalized difference vegetation index (NDVI): unforeseen successes in animal ecology. Clim Res 46(1):15–27

Pettorelli N, Laurance WF, O'Brien TG, Wegmann M, Nagendra H, Turner W (2014a) Satellite remote sensing for applied ecologists: opportunities and challenges. J Appl Ecol 51(4):839–848

Pettorelli N, Safi K, Turner W (2014b) Satellite remote sensing, biodiversity research and conservation of the future. Philos Trans Royal Soc Lond b: Biol Sci 369(1643):20130190

Pfeifer M, Disney M, Quaife T, Marchant R (2012) Terrestrial ecosystems from space: a review of earth observation products for macroecology applications. Global Ecol Biogeogr 21(6):603–624

Polgar CA, Primack RB (2011) Leaf-out phenology of temperate woody plants: from trees to ecosystems. New Phytol 191(4):926–941

Pomara LY, Lee DC (2021) The role of regional ecological assessment in quantifying ecosystem services for forest management. Land 10(7):725

Ponti R, Sannolo M (2022) The importance of including phenology when modelling species ecological niche. Ecography 2023:e06143

Quinlan AE, Berbés-Blázqusez M, Haider LJ, Peterson GD (2016) Measuring and assessing resilience: broadening understanding through multiple disciplinary perspectives. J Appl Ecol 53(3):677–687

R Core Team (2021) R: A language and environment for statistical computing. R Foundation for Statistical Computing, Vienna, Austria. http://www.R-project.org

Radeloff VC, Dubinin M, Coops NC et al (2019) The Dynamic Habitat Indices (DHIs) from MODIS and global biodiversity. Remote Sens Environ 222:204–214

Reed BC, Brown JF, VanderZee D, Loveland TR, Merchant JW, Ohlen DO (1994) Measuring phenological variability from satellite imagery. J Veg Sci 5(5):703–714

Rieb JT, Chaplin-Kramer R, Daily GC et al (2017) When, where, and how nature matters for ecosystem services: challenges for the next generation of ecosystem service models. Bioscience 67(9):820–833

Riitters KH, Wickham JD, Wade TG (2009) An indicator of forest dynamics using a shifting landscape mosaic. Ecol Indic 9(1):107–117

Riitters K, Schleeweis K, Costanza J (2020) Forest area change in the shifting landscape mosaic of the continental United States from 2001 to 2016. Land 9(11):417

Riitters K, Costanza JK, Coulston JW, Vogt P, Schleeweis K (2023) Interpreting image texture metrics applied to landscape gradient data. Landsc Ecol 38(9):2179–2188

Rutledge RW, Basore BL, Mulholland RJ (1976) Ecological stability: an information theory viewpoint. J Theor Biol 57(2):355–371

Scheffer M, Carpenter S, Foley JA, Folke C, Walker B (2001) Catastrophic shifts in ecosystems. Nature 413(6856):591–596

Seidl R, Spies TA, Peterson DL, Stephens SL, Hicke JA (2016) Searching for resilience: addressing the impacts of changing disturbance regimes on forest ecosystem services. J Appl Ecol 53(1):120–129

Shannon CE (1948) A mathematical theory of communication. Bell Syst Tech J 27:379–423

Silveira EMO, Radeloff VC, Martínez Pastur GJ et al (2022) Forest phenoclusters for Argentina based on vegetation phenology and climate. Ecol Appl 32(3):e2526

Smith HG, Sheridan GJ, Lane PNJ, Nyman P, Haydon S (2011) Wildfire effects on water quality in forest catchments: a review with implications for water supply. J Hydrol 396(1):170–192

Spies TA, Turner MG (1999) Dynamic forest mosaics. In: Hunter ML (ed) Maintaining biodiversity in forest ecosystems. Cambridge University Press, Cambridge, pp 95–160

Spruce JP, Sader S, Ryan RE et al (2011) Assessment of MODIS NDVI time series data products for detecting forest defoliation by gypsy moth outbreaks. Remote Sens Environ 115(2):427–437

Spruce JP, Hicke JA, Hargrove WW, Grulke NE, Meddens AJH (2019) Use of MODIS NDVI products to map tree mortality levels in forests affected by Mountain Pine Beetle outbreaks. Forests 10(9):811

Spruce JP, Gasser GE, Hargrove WW (2016) MODIS NDVI data, smoothed and gap-filled, for the conterminous US: 2000-2015. ORNL DAAC, Oak Ridge, Tennessee, USA. https://doi.org/10.3334/ORNLDAAC/1299

Steuer R, Kurths J, Daub CO, Weise J, Selbig J (2002) The mutual information: detecting and evaluating dependencies between variables. Bioinformatics 18(suppl 2):S231–S240

Trumbore S, Brando P, Hartmann H (2015) Forest health and global change. Science 349(6250):814–818

Ulanowicz RE (1986) Growth and development: ecosystems phenomenology. Springer, Cham

Ulanowicz RE (1997) Ecology, the ascendent perspective. Columbia University Press, New York

Ulanowicz RE (2003) Some steps toward a central theory of ecosystem dynamics. Comput Biol Chem 27(6):523–530

Ulanowicz RE (2009) A third window: natural life beyond Newton and Darwin. Templeton Foundation Press, West Conshohocken

Ulanowicz RE, Goerner SJ, Lietaer B, Gomez R (2009) Quantifying sustainability: resilience, efficiency and the return of information theory. Ecol Complex 6(1):27–36

Vandermeer J (1981) Elementary mathematical ecology. John Wiley and Sons, New York

Vose JM, Wear DN, Mayfield AE, Nelson CD (2013) Hemlock woolly adelgid in the southern Appalachians: control strategies, ecological impacts, and potential management responses. For Ecol Manage 291:209–219

Wang J, Zhang X (2020) Investigation of wildfire impacts on land surface phenology from MODIS time series in the western US forests. ISPRS J Photogramm Remote Sens 159:281–295

Wang C, Zhao H (2018) Spatial heterogeneity analysis: Introducing a new form of spatial entropy. Entropy 20(6):398

Weber KT, Yadav R (2020) Spatiotemporal trends in wildfires across the Western United States (1950–2019). Remote Sens 12(18):2959

Weiskopf SR, Rubenstein MA, Crozier LG et al (2020) Climate change effects on biodiversity, ecosystems, ecosystem services, and natural resource management in the United States. Sci Total Environ 733:137782

Wu J (2013) Landscape sustainability science: ecosystem services and human well-being in changing landscapes. Landscape Ecol 28(6):999–1023

Wu J, Loucks OL (1995) From balance of nature to hierarchical patch dynamics: a paradigm shift in ecology. Q Rev Biol 70:439–466

Zaccarelli N, Li B-L, Petrosillo I, Zurlini G (2013) Order and disorder in ecological time-series: introducing normalized spectral entropy. Ecol Indicators 28:22–30

Zhang X, Friedl MA, Schaaf CB et al (2003) Monitoring vegetation phenology using MODIS. Remote Sens Environ 84(3):471–475

Zhang X, Liu L, Henebry GM (2019) Impacts of land cover and land use change on long-term trend of land surface phenology: a case study in agricultural ecosystems. Environ Res Lett 14(4):044020